Analysis of the generation potential of hybrid solar power plants

Gleyzer Martins[1]*, Oscar Saul Hernandez Mendoza[1], Muhammad Amjad[2] and Enio Pedone Bandarra Filho[1]*

[1]School of Mechanical Engineering, Federal University of Uberlandia, Uberlandia, Brazil, [2]Department of Mechanical, Mechatronics and Manufacturing Engineering, New Campus, University of Engineering and Technology Lahore, Lahore, Pakistan

Photovoltaic solar energy has emerged in Brazil in distributed generation due to affordable costs and its application in different segments of the market. However, the electric energy storage in the photovoltaic systems is only viable for certain conditions in which the installation does not have access to the electricity network and the thermal portion of the solar energy is lost to the ambient. Heliothermic power plant represents another system available for solar electricity generation, which has higher costs, but takes better advantage of the portion of thermal energy and allows energy storage efficiently to meet the demands during periods without incident solar radiation. Heliothermic and photovoltaic generation have great potential in the Southeast and Northeast regions of Brazil, but the costs of both technologies cannot meet the demands during periods without solar radiation. This work presents a conceptual analysis of compound parabolic solar concentrators along with hybrid of photovoltaic and thermal collector systems to meet both the demand during sunlight hours and without solar radiation. The investigation consisted of implementing an organic Rankine cycle with different heliothermic plant configurations and the analysis of the diode model to examine different commercial photovoltaic cells operated in the Rankine cycle evaporation region. The results showed that the best working fluid for the application is R245fa with Urea–NaCl as molten salt for the thermal energy storage. The expected electrical power for the hydride cycle is 1580W at 2600 rpm and at 80°C of evaporation temperature, enabling a power generation for 1 hour and 20 min without solar radiation.

KEYWORDS

photovoltaic, heliothermic, heat storage, molten salt, hybrid power plant

1 Introduction

The use of solar concentration in monocrystalline photovoltaic modules results in significant improvements in electricity generation, as long as the effects of operating temperature on cell performance are considered (O'Gallagher, 2008). Notably, the amount solar energy that is not converted in these applications can reach more than 80% of the incident energy.

Studies of hybrid photovoltaic-thermal systems for heat and electricity generation have shown promising results in the existing literature (Khelifa et al., 2015; Tae-Hyeon et al. (2017). Hybrid power plants are described in the literature in practically three ways: photovoltaic/thermal hybrid solar systems for heat extraction (Tripanagnostopoulos et al., 2002; Coventry, 2005; Rosell et al., 2005; Chow, 2010); photovoltaic plants and

thermoelectric materials for electricity generation (Vorobiev et al., 2006); and photovoltaic systems and organic Rankine cycles for power production (Manolakos and Papadakis, 2011; Tourkov and Schaefer, 2015; Hosseini and Butler, 2021).

Organic Rankine cycles operate in low temperature using an organic working fluid. According to Tourkov and Schaefer (2015), this cycle can operate with dry fluids (n-Pentane), wet fluids (Ammonia), and isentropic fluids (R11). These categories are associated to the vapor saturation curve, where dry fluids have a positive slope, wet fluids a negative one and isentropic nearly vertical one. It is important to highlight that for low-temperature organic Rankine cycles the dry fluids are recommended, since the outlet of the turbine is guaranteed to be in the superheated vapor region (Tourkov and Schaefer, 2015).

Different working fluids, several configurations of organic Rankine cycle and photovoltaic cell types were evaluated to improve photovoltaic thermal/organic Rankine cycle systems (Tourkov and Schaefer, 2015). The findings revealed that alkanes (n-butane) performed best in terms of efficiency, and the advanced configuration using internal heat exchanger (IHE) and a closed feed organic fluid heater (CFOH) was the best match for these operating fluids. Additionally, the CdS photovoltaic cells were the least affected by increasing operating temperature on the photovoltaic system.

Experimental investigation and simulation developed by Kosmadakis, Manolakos and Papadakis (2011) also demonstrated that the efficiency of hybrid power plants can reach up to 12%, with emphasis for R-245fa as a working fluid, in addition to pointing out that hybrid systems have better economic feasibility than concentrating photovoltaic systems.

With hybrid power plants, it is possible to use both direct photovoltaic energy and fraction of the heat rejected for thermoelectric power generation. Another valuable aspect is the development of heliothermic power plants that, despite the remarkable potential, is still little explored in Brazil, as described in the online platform Heliothermic, supported by the Brazilian Institute of Information in Science and Technology.

Heliothermic power plants convert solar energy into thermal energy, producing mechanical power for electricity generation through a thermal cycle. Usually, thermal cycles are based on the organic Rankine cycle, that uses solar energy to vaporize and superheat the working fluid (synthetic oils, molten salt or water vapor) (Tolmasquim, 2016), which when expanding in a turbine or expander coupled to an electrical generator, produces electricity. To close the cycle, a heat exchanger, condenser (to condense the working fluid) and a pump are used.

Heliothermic power plant's net electrical energy output represents just 16% of the incident solar energy, owing to low temperatures and efficiency of heat transfer to the fluid in the receiver (Schmalensee et al. (2015)).

The arrangements for concentrating solar energy in the heliothermic power plants are classified in point-focus or line-focus designs, in which the receiving fluid can be fixed or mobile, allowing four types of configurations: linear Fresnel (line-focus design and fixed fluid); solar tower (point-focus design and fixed fluid; parabolic trough (line-focus design and mobile fluid) and parabolic receiver system (point-focus design and mobile fluid).

The photovoltaic systems available on the market can be differentiated according to the absorption spectrum of solar radiation, in single-junction and multi-junction photovoltaic cells. The absorption spectrum of single-junction solar cells is smaller, with silicon monocrystalline cells being the most commercially efficient, although the market offers other technologies, including thin-film polycrystalline cadmium telluride (CdTe) solar cells, copper-indium-gallium diselenide (CIGS) and hydrogenated amorphous silicon (a-Si:H). In general, the efficiency of commercial single-junction cells is below 21%, with acquisition costs increasingly accessible to end consumers. The absorption spectrum of multi-junction cells is broader, allowing better efficiency, in the order of 40%, requiring solar cell under high light concentration to maximize conversion into electrical energy (Dambhare, Butey, Moharil, 2021). The solar concentration associated with the solar tracking system increases the costs of installing multi-junction cells, thereby limiting the economic feasibility of this technology.

The application of concentrating photovoltaic cells, despite increasing the electrical generation per cell and reducing costs with expensive materials, such as high-purity silicon, can be negatively affected, as solar concentration can reduce its life span.

The research problem is to evaluate what is the configuration for the photovoltaic system and for the organic Rankine cycle with thermal storage that enhances the application of a hybrid solar plant. The present work seeks to evaluate the best types of commercial photovoltaic cells and the configuration of the Organic Rankine cycle, where different working fluids, operating conditions and different fusible salts of the thermal reservoir that enhance the electrical generation of a hybrid solar plant are studied. Thus, the theoretical electrical generation of the organic Rankine cycle was modeled with the scroll expander model defined by Lemort et al. (2006) and the diode modeling was carried out to quantify the electrical generation of photovoltaic cells.

The use of the hybrid cycle will improve the electrical generation of photovoltaic cells by using solar concentration and by reducing the operating temperature of these cells due to the use of the saturation region of the Organic Rankine cycle. The Organic Rankine cycle will also increase electrical generation, in addition to enabling the thermal storage of energy to be used in electrical generation outside the period of insolation.

2 Methodology

The photovoltaic and heliothermal plant consists of parabolic concentrators that concentrate solar energy 4.5 times under a linear array of photovoltaic cells. This cell arrangement was installed on an aluminum plate in the saturation region of the organic Rankine cycle, an additional cellless collector area was employed to superheat the working fluid entering the thermal storage tank. In the storage tank, part of the thermal energy is stored using fusible salts and another part directed to the scroll expander for electrical generation. This working fluid at the outlet of the expander is condensed in the heat exchanger for subsequent pumping, closing the organic Rankine cycle. Figure 1 presents the proposed hybrid solar plant.

For the photovoltaic analysis and determination of the solar collector areas, the standard irradiation of 1000 W/m^2 was considered. The power generation performance of photovoltaic cells was evaluated using the diode model for the photovoltaic cells

FIGURE 1
Schematic representation of the proposed hybrid solar system.
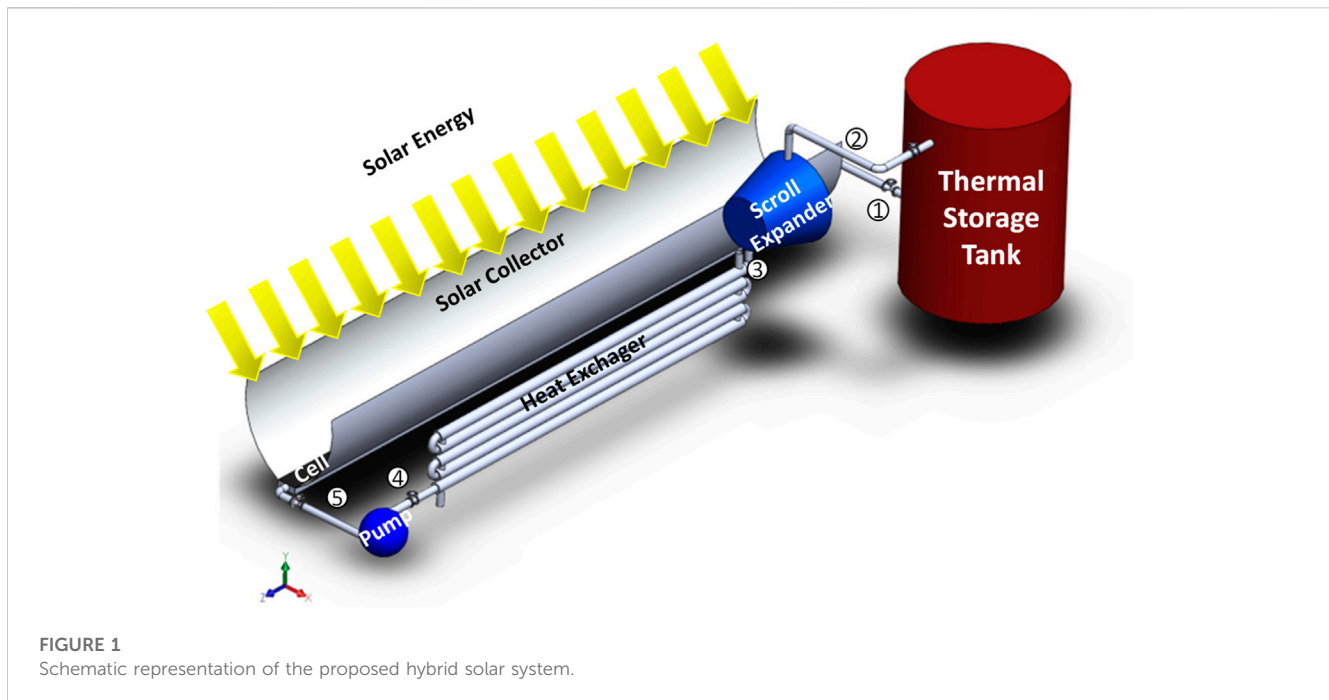
and electricity data of the single-junction cells, since it is necessary to calculate the effect of temperature on the efficiency of cells.

For the analysis of the organic Rankine plant, the operating pressures were defined according to the different temperatures in the evaporator, keeping the temperature in the condenser at 35°C, and the temperature at the outlet of the evaporator and at the inlet of the storage tank is equal to 150°C. A scroll expander derived was implemented from the scroll compressor with 36.54 cc and the parameters defined by Lemort et al. (2009).

The modeling of hybrid power plant was divided into models for simulating the heliothermic power plant, especially the expander model, and for simulating photovoltaic electricity generation. An analysis of the hybrid plants available in the literature was also performed. The modeling of the heliothermic power plant used the conservation of mass and energy applied to the basic equipment of the organic Rankine cycle, pump, expander and heat exchangers, according to Landellea et al. (2017) and Equations 1, 2:

$$0 = \frac{d}{dt} \int_{cv} \rho dv + \int_{cs} \rho(\vec{V} \cdot \vec{n}) dA \qquad (1)$$

$$\dot{Q} - \dot{W} = \frac{d}{dt} \int_{cv} \rho\left(u + \frac{V^2}{2} + z\right) dv + \int_{cs} \rho\left(h + \frac{V^2}{2} + z\right)(\vec{V} \cdot \vec{n}) dA \qquad (2)$$

The system's simulation was performed at a steady-state condition, and the equipment was modeled theoretically at a constant performance, except for the expander. The model proposed by Lemort et al. (2006) and Lemort, Declaye and Quoilin (2011) was used to simulate the expander, which consists of determining the power developed by the expander considering the heat exchanges with the environment and the expansion process in two stages, one isentropic and another isovolumetric, considering that total power is theoretical power plus losses, as illustrated in Figure 2.

The mass flow rate is a function of the expander swept volume V_s, the compressor rotational speed N, and leakages $\dot{M}_{leak}$ (Equation 3):

$$\dot{M} = \frac{N \cdot V_S}{v_{su,2}} + M_{leak} \qquad (3)$$

The internal expansion power $\dot{W}_{in}$, is calculated using an isentropic expansion and a constant-volume evolution, according to Eq. 4:

$$\dot{W}_{in} = \dot{M}_{in}\left[(h_{su,2} - h_{ad}) + r_{v,in} \cdot v_{su,2}(P_{ad} - P_{ex,2})\right] \qquad (4)$$

where $h_{su,2}$ and h_{ad} are the enthalpies of the fluid at the supply of the expander and of the isentropic expansion, respectively, and $P_{ex,2}$ and P_{ad} represent the exhaust pressure and isentropic expansion pressures. $r_{v,in}$ is the internal volume ratio.

The total power $\dot{W}$ is computed considering the power losses due to mechanical losses $\dot{W}_{loss,1}$ and electromechanical losses $\dot{W}_{loss,2}$ as defined by Eq. 5.

$$\dot{W} = \dot{W}_{in} - \dot{W}_{loss,1} - W_{loss,2} \qquad (5)$$

Internal heat transfers are lumped into equivalent supply $\dot{Q}_{su}$ and exhaust $\dot{Q}_{ex}$ heat rates, based on overall heat transfer coefficients, while external heat transfer is also defined by a global heat transfer coefficient AU_{amb}, and the energy balance can be given by Eq. 6:

$$Q_{su} + \dot{Q}_{ex} - AU_{amb} \cdot (T_{Shell} - T_{amb}) + \dot{W}_{loss,1} + \dot{W}_{loss,2} = 0 \qquad (6)$$

where T_{Shell} and T_{amb} represent the temperatures associated to the expander shell and the ambient, respectively.

To estimate the generation of photovoltaic cells, the effect of temperature on the efficiency of solar cells must be calculated, which, according to Gow and Manning, (1999), is given by the diode model, as defined below:
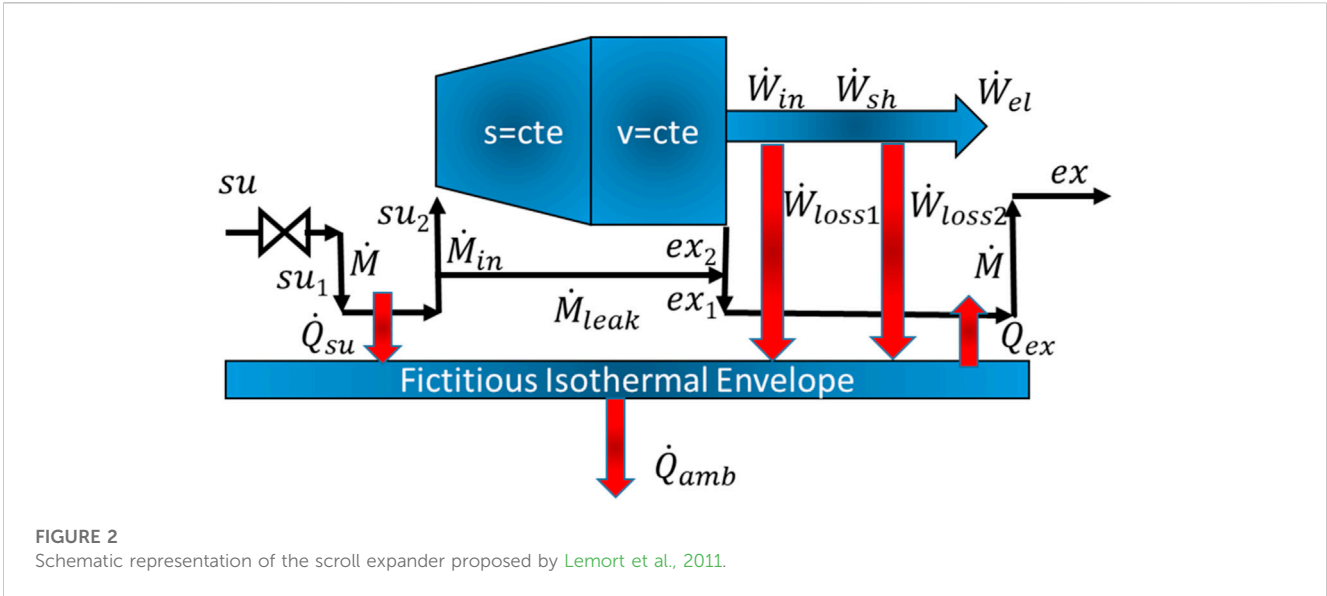
FIGURE 2
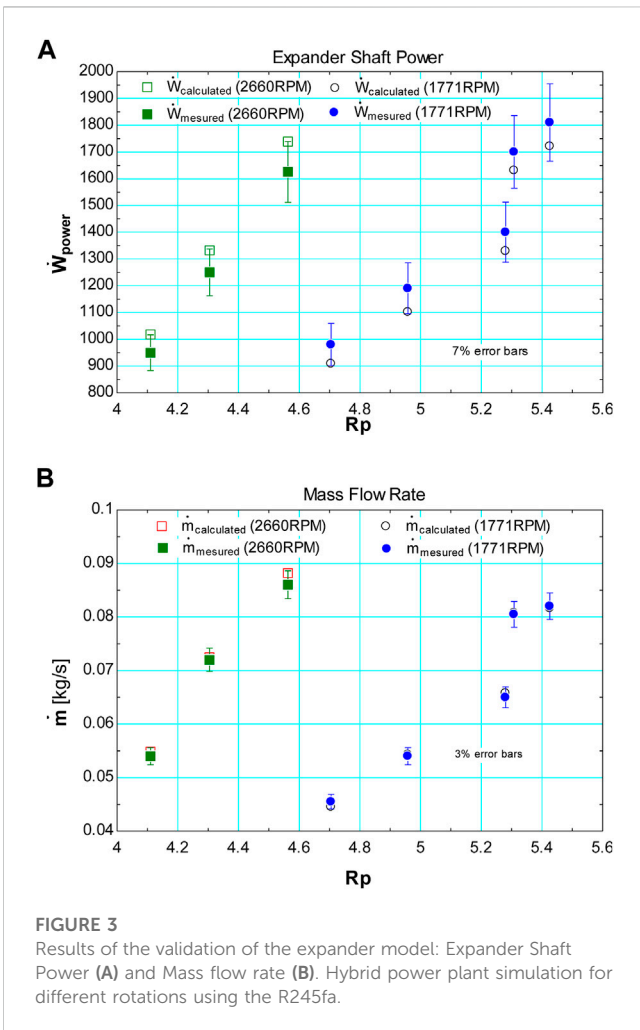Schematic representation of the scroll expander proposed by Lemort et al., 2011.

FIGURE 3
Results of the validation of the expander model: Expander Shaft Power **(A)** and Mass flow rate **(B)**. Hybrid power plant simulation for different rotations using the R245fa.

$$I = I_{fg} - I_0 \times \left[\exp\left(\frac{(V + R_s \times I)}{n \times k \times T} \right) - 1 \right] \qquad (7)$$

$$I_{fg} = [I_{cc} + \alpha \times (T - T_r)] \times \frac{S}{S_r} \qquad (8)$$

$$I_0 = \frac{I_{fg}}{\left(\exp\left(\frac{V_{ca} \times q}{n \times k \times T} \right) - 1 \right)} \exp\left(\frac{q \times EG}{n \times k} \times \left(\frac{1}{T_r} - \frac{1}{T} \right) \right) \qquad (9)$$

In these equations, I_{fg}, I_0 and I_{cc} represent the output, photogenerated, diode saturation and short-circuit currents, respectively; V and V_{Ca} are the terminal and open-circuit voltages; T and T_r are the module and standard module temperatures; S and S_r are the intensities of solar radiation and standard solar radiation. The model constants are α, k, n, q and EG, which represent the temperature coefficient, the Boltzmann constant, the diode ideality factor, the elementary charge and the energy band-gap, respectively. The series resistance, R_s, is a parameter that adjusts the model to the modules used. The effects of temperature and variation of solar irradiation are considered in the photogenerated current and in the diode saturation current (GOW AND MANNING, 1999).

3 Results and discussions

Initially, the results of mass flow and shaft power of the scroll expander were validated for different pressure ratios and rotational speeds, according to data from Lemort et al. (2009), as shown in Figure 3.

Figure 3A illustrates that the scroll expander model predicts, satisfactorily, the mass flow rate with errors smaller than 3%. However, Figure 3B shows the increment of errors in the shaft power expander simulation approximately of 7%. The Lemort et al. (2009) presents similar errors in the prediction experimental mass flow and shaft power for scroll expander.

To evaluate the effect of the working fluid on the hybrid power plant, a simulation of the operating conditions of the heliothermal and photovoltaic power plant was performed, considering a standard Rankine cycle and temperature conditions of 75°C in

TABLE 1 Results for different refrigerants as working fluid.

	R11	R123	R245fa	R134A	R1234yf	R423A
$\dot{m}_{ref}$ [KG/S]	0.02551	0.0264	0.03837	0.114	0.1239	0.1253
$Area_{colector}$ [M^2]	6.819	7.332	12.4	34.07	33.89	32.68
$Area_{Phovoltaic}$ [M^2]	4.891	4.812	7.691	20.65	18.37	18.49
$Pressure_{Evaporator}$ [BAR]	1.479	1.307	2.11	8.875	8.952	7.965
$Pressure_{Condenser}$ [BAR]	4.594	4.31	6.958	23.66	22.72	21.42
$Power_{photovoltaic}$ [W]	409	402.4	643.2	1,727.4	1,536.6	1,546.8
$Power_{Rankine}$ [W]	110.7	174.9	335.1	378.1	317.3	569.7
$Power_{Total}$ [W]	510.6	568.1	954.7	1,865.0	1,584.1	1,889.6
η_{total} [%]	10.13	10.96	11.31	9.575	9.385	10.27

the evaporator tube and 30 °C in the condenser tube. The results are depicted in Table 1.

Table 1 shows that the choice of operating fluid is important for defining the areas of solar capture and application of solar cells and for determining the power generation performance of the thermal plant. The working fluids R134a, R1234yf and R423A, in other words, high pressure fluids, require the largest areas of solar energy collection, as these larger areas provide a greater power of the hybrid system, mainly the photovoltaic portion. In turn, the working fluids R11, R123 and R245fa (low pressure fluids) have the smallest areas of solar energy collection and, consequently, the smallest photovoltaic power. However, these fluids demonstrate the best thermal efficiencies for the hybrid system, especially R245fa, which showed better thermal efficiency with heliothermal power similar to the fluids with large energy collection area. As the photovoltaic-cell operating temperatures are constant for the different fluids, a result of the photovoltaic efficiency of 8.364% was achieved.

In terms of pressures in the cycles, it can be observed that the fluids with smaller areas of solar capture have the lowest pressures, which reduces the thickness of pipes and pressure vessels, hence reducing costs.

Thus, analyzing in detail the simulations of the thermal fluid R245fa for different rotations, it is possible to obtain Figure 3.

Figure 3B illustrates that the power and efficiency in the hybrid cycle increase significantly with increasing rotation, showing a clear trend of efficiency stabilization. Particularly, in Figure 3A, it is possible to observe the increase of collector area and mass flow rate.

Figure 4 shows the simulation of the hybrid power plant, evaluating the effect of molted salt type in accordance of thermo-physical properties defined by Sabour and Dorca (2019).

Figure 4 also shows that best molted-salts efficiency and solar collect area is the KNO3NaNO2, since this salt present the lowest electric power and operation time of power plant without incident solar radiation. The Urea-NaNO3 represents the molted salt with high electric power, however lowest efficiency and high solar collect area. The Urea-NaCl and Urea-KCl show moderate solar collect area with satisfactory electric power, efficiency and operation time, although the efficiency of Urea-KCl is better than Urea-NaCl, the cost and commercial availability is favorable in the Urea-NaCl choice.
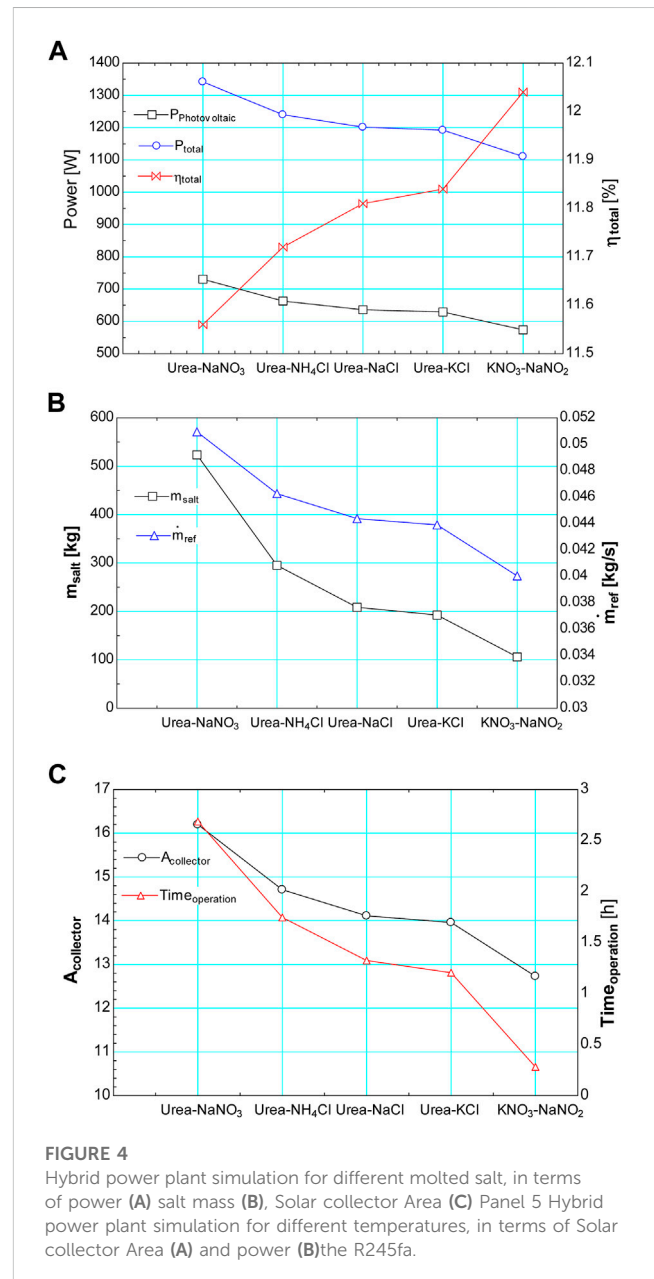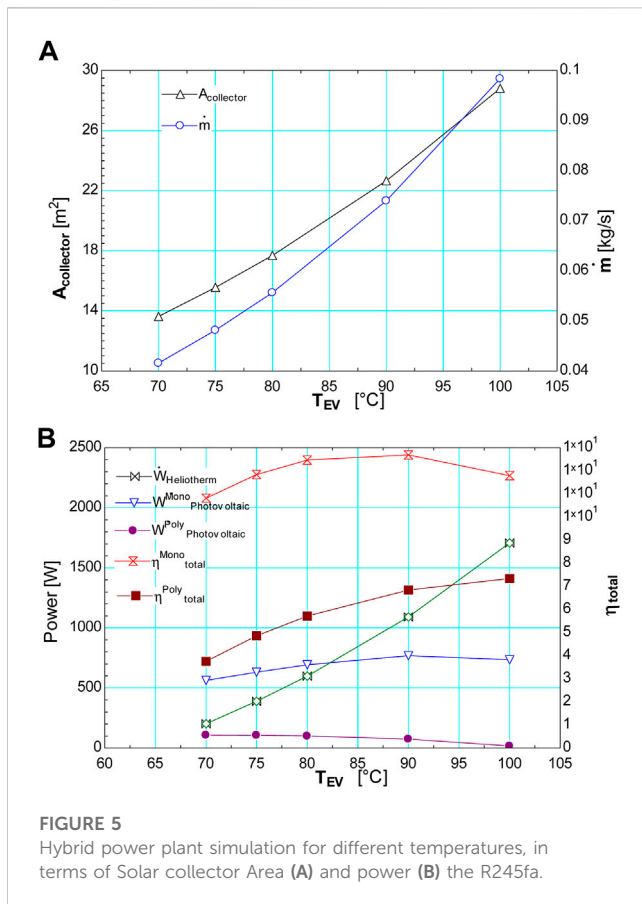

FIGURE 4
Hybrid power plant simulation for different molted salt, in terms of power **(A)** salt mass **(B)**, Solar collector Area **(C)** Panel 5 Hybrid power plant simulation for different temperatures, in terms of Solar collector Area **(A)** and power **(B)** the R245fa.

FIGURE 5
Hybrid power plant simulation for different temperatures, in terms of Solar collector Area **(A)** and power **(B)** the R245fa.

To determine the influence of the evaporation temperature, that is, the operating temperature of the two different commercial photovoltaic cells, it was possible to obtain Figure 5.

Figure 5 shows that the increment in evaporation temperature increases the solar collector area and the mass flow rate, as well as the heliothermic power. However, it can be noted a marked reduction of the photovoltaic power and a peak of efficiency at 80 ˚C for monocrystalline cells. The polycrystalline cells, in turn, present results of low photovoltaic energy generation and consequent low efficiency of the hybrid cycle.

Based on experimental results, the optimum operating point of the system is with a rotation of 2600 rpm and an evaporation temperature of 80 ˚C, with a hybrid cycle performance of 12% and a total power of 1580W. The cycle also achieved higher powers using monocrystalline cells, at the expense of photovoltaic power and cycle efficiency. Thus, a solar collector area of 17.68 m^2 is recommended, which requires a salt storage of 261.3 kg and an operating time without incident solar radiation of 1h20min.

4 Conclusion

Photovoltaic solar energy is widespread due to the affordable costs of installations and abundant availability. Non-etheless, this system presents problems with its storage, both due to the direct and indirect costs of batteries. In turn, the

proposal of a hybrid heliothermic and photovoltaic plant represents a way to extend the use of solar energy to periods without solar radiation with the storage of thermal energy in fusible salts. Further, the heliothermic system allows thermal protection of concentrating solar cells in the biphasic heat exchange region. In this sense, different working fluids were evaluated for a heliothermic power plant operating with an organic Rankine cycle, using a scroll expander to generate electricity. Moreover, different media for solar thermal energy storage including fusible salts, urea and common salt were investigated for extended periods without solar radiation. As per the numerical results, the best working fluid for the installation of the hybrid solar plant was R245fa, using monocrystalline cells and Urea-NaCl molted salt as storage material with a recommended solar concentration area of 17.7 m^2. An increased operation time of 1 h and 20min for power generation was observed thus making the system a viable solution for operation in the absence of the solar flux.

Author contributions

GM conducted all the simulations and analyses, OM contributed with the simulation as well as the results analyses. MA performed the revision and revision the manuscript and EB organized the material, written and participes the discussion.

References

Chow, T. T. (2010). A review on photovoltaic/thermal hybrid solar technology. *Appl. Energy* 87, 365–379. doi:10.1016/j.apenergy.2009.06.037

Coventry, J. S. (2005). Performance of a concentrating photovoltaic/thermal solar collector. *Sol. Energy* 78, 211–222. doi:10.1016/j.solener.2004.03.014

Dambhare, M. V., Butey, B., and Moharil, S. V. (2021). Solar photovoltaic technology: A review of different types of solar cells and its future trends. *J. Phys. Conf. Ser.* 1913, 012053. doi:10.1088/1742-6596/1913/1/012053

Gow, J. A., and Manning, C. D. (1999). Development of a photovoltaic array model for use in power-electronics simulation studies. *IEE Proc.* 146, 193. doi:10.1049/ip-epa:19990116

Hosseini, S. E., and Butler, B. (2021). Design and analysis of a hybrid concentrated photovoltaic thermal system integrated with an organic Rankine cycle for hydrogen production. *J. Therm. Analysis Calorim.* 144, 763–778. doi:10.1007/s10973-020-09556-4

Khelifa, A., Touafek, K., Ben Moussa, H., Tabet, I., Ben cheikh El hocine, H., and Haloui, H. (2015). Analysis of a hybrid solar collector photovoltaic thermal (PVT). *Energy Procedia* 74, 835–843. doi:10.1016/j.egypro.2015.07.819

Landellea, A., Tauverona, N., Haberschillc, P., Revellinc, R., and Colassona, S. (2017). Performance evaluation and comparison of experimental organic rankine cycle prototypes from published data. *Procedia* 105, 1706–1711. doi:10.1016/j.egypro.2017.03.555

Lemort, V., Declaye, S., and Quoilin, S. (2011). Experimental characterization of a hermetic scroll expander for use in a micro-scale Rankine cycle. *Part A J. Power Energy* 226, 126–136. doi:10.1177/0957650911413840

Lemort, V., Quoilin, S., Cuevas, C., and Lebrun, J. (2009). Testing and modeling a scroll expander integrated into an organic Rankine cycle. *Appl. Therm. Eng.* 29, 3094–3102. doi:10.1016/j.applthermaleng.2009.04.013

Lemort, V., Teodorese, I. V., and Lebrun, J. (2006). *Experimental study of the integration of a scroll expander into a heat recovery rankine cycle*. International Compressor Engineering Conference.

Manolakos, D., and Papadakis, G. (2011). Simulation and economic analysis of a CPV/thermal system coupled with an organic Rankine cycle for increased power generation. *Sol. Energy* 85, 308–324. doi:10.1016/j.solener.2010.11.019

O'Gallagher, J. J. (2008). "Practical design of CPC PV concentrators," in *Nonimaging optics in solar energy. Synthesis lectures on energy and the environment: Technology, science, and society* (Cham: Springer). doi:10.1007/978-3-031-79420-9_4

Rosell, J. I., Vallverdú, X., Lechón, M. A., and Ibánez, M. (2005). Design and simulation of a low concentrating photovoltaic/thermal system. *Energy Convers. Manag.* 46, 3034–3046. doi:10.1016/j.enconman.2005.01.012

Sabour, I., and Dorca, A. (2019). Review on heat transfer analysis in thermal energy storage using latent heat storage systems and phase change materials. *Int. J. Energy Res.* 43, 29–64. doi:10.1002/er.4196

Schmalensee, R., Bulovic, V., Armstrong, R., Batlle, C., Brown, P., Deutch, J., et al. (2015). *The future of solar energy: An interdisciplinary MIT study*. Massachusetts Institute of Technology, MIT Energy Initiative.

Tae-Hyeon, K., Kim, S., Jeong, D. H., Geum, D. M., Lee, S., Junga, S. J., et al. (2017). A highly-efficient, concentrating-photovoltaic/thermoelectric hybrid generator. *Nano Energy* 37, 242–247. doi:10.1016/j.nanoen.2017.05.023

Tolmasquim, M. T. (2016). *Energia renovável: Hidráulica, biomassa, eólica, solar, oceânica*. Rio de Janeiro: EPE.

Tourkov, T., and Schaefer, L. (2015). Performance evaluation of a PVT/ORC (photovoltaic thermal/organic Rankine cycle) system with optimization of the ORC and evaluation of several PV (photovoltaic) materials. *Energy* 82, 839–849. doi:10.1016/j.energy.2015.01.094

Tripanagnostopoulos, Y., Nousia, Th., Souliotis, M., and Yianoulis, P. (2002). Hybrid photovoltaic/thermal solar systems. *Sol. Energy* 72, 217–234. doi:10.1016/s0038-092x(01)00096-2

Vorobiev, Yu., González-Hernández, J., Vorobiev, P., and Bulat, L. (2006). Thermal-photovoltaic solar hybrid system for efficient solar energy conversion. *Sol. Energy* 80, 170–176. doi:10.1016/j.solener.2005.04.022

Nomenclature

A Area [m^2]

E energy band-gap [eV]

k Boltzmann constant [J/K]

$\dot{M}$ Mass flow [kg/s]

$\vec{n}$ Unit Vector

n diode ideality factor

$\dot{Q}$ Heat transfer [W]

R_s Series resistance [Ω]

T Temperature [K]

V Voltages [V]

v Specific Volume [m^3/kg]

z Elevation [m]

AU Global heat transfer coefficient [W/m^2-K]

h Enthalpy [kJ/kg]

I Circuit current [A]

N Rotation [rpm]

P Pressure [Bar]

r_v Internal volume ration

S Solar radiation Intensity [W/m^2]

u Internal energy[kJ/kg]

$\vec{V}$ Velocity [m/s]

V_s Swept volume [m^3]

$\dot{W}$ Power [W]

Subscribed

ad Adiabatic

ca Open-circuit t

cv Control volume

ex Exhaust

fg Photogenerated

$leak$ Leakages

o Diode saturation

$shell$ Shell

amb Ambient

cc Circuit curren

cs Control surface

el Electric

in Internal

$loss$ Losses

r Standard

su Supply

Greek Symbols

ρ Density [kg/m^3]

α Temperature Coefficient [1/K]